Robust control pulses design for electron shuttling in solid state devices

Jun Zhang[1,2], Loren Greenman[2], Xiaotian Deng[2], and K. Birgitta Whaley[2]
[1] *Joint Institute of UMich-SJTU, Shanghai Jiao Tong University, and Key Laboratory of System Control and Information Processing, Ministry of Education, Shanghai, 200240, China*
[2] *Department of Chemistry, Berkeley Center for Quantum Information and Computation, University of California, Berkeley, California 94720, USA*
(Dated: October 10, 2012)

In this paper we study robust pulse design for electron shuttling in solid state devices. This is crucial for many practical applications of coherent quantum mechanical systems. Our objective is to design control pulses that can transport an electron along a chain of donors, and also make this process robust to parameter uncertainties. We formulate it as a set of optimal control problems on the special unitary group SU(n), and derive explicit expressions for the gradients of the aggregate transfer fidelity. Numerical results for a donor chain of ionized phosphorus atoms in bulk silicon demonstrate the efficacy of our algorithm.

I. INTRODUCTION

Recent years have witnessed the rapid advance of solid state devices that take full advantage of coherent quantum mechanical properties [1–5]. One particular application of such devices is quantum computation, which has attracted intensive research interest over the past 15 years. To implement these devices in practical applications, a central task is to generate a quantum state transfer. For example, it is often desired to transfer the population between different energy levels or different spatial locations so that quantum information can be circulated and processed on a large scale.

In this paper we consider the design of robust control pulses for coherent electron shuttling in solid state devices with a one-dimensional array of quantum dots or donors. There are a number of proposals which use the donated electron of Group V dopants such as phosphorus in silicon as qubits [1–3]. Such dopants can be inserted using ion implantation [6–8]. Recently developed techniques using a scanning tunneling microscope have further allowed them to be placed with high precision [8, 9]. In order to couple donors and achieve greater scalability of qubit array size, it is desirable to be able to move qubits robustly between distant physical locations [2]. The objective is to transport the electron along a chain of donors so that the encoded quantum information can be communicated between distant qubits. Specifically, at the beginning of this procedure, an electron is localized at one end of the chain. Then by applying some appropriate external control fields, we seek to shuttle the electron to the other end of the chain. Depending on the specific physical implementation, the control fields can be gate voltage [10, 11] or tunable on-site energy [12].

To achieve such electron shuttling, Greentree et al. [10] have proposed to use a solid state version of the well-known Stimulated Raman Adiabatic Passage (STIRAP) for population transfer in quantum optics [13, 14]. In this adaptation to the solid state, which is known as Coherent Tunneling Adiabatic Passage (CTAP), two Gaussian pulses are applied in a *counter-intuitive* sequence to realize the population transfer in an adiabatic manner, *i.e.*, starting in an eigenstate of the system Hamiltonian and changing the Hamiltonian sufficiently slowly so that the system will remain in the corresponding eigenstate during the entire transfer process. The amplitudes, peak times, and standard deviations of the two CTAP pulses have to be carefully tuned. We have recently shown that adiabaticity is, however, not a requisite condition for achieving high fidelity electron shuttling between spatial locations. In Ref. [15], we have applied Lie-Poisson reduction to develop a geometric control approach to remove the adiabatic condition and to accomplish the quantum state transfer with complete fidelity.

In the current paper we are interested in the design of control pulses for electron shuttling that are robust with respect to relevant experimental parameters. In many experiments it is inevitable that some physical parameters are not precisely known although we may have confidence that they lie in a certain range. This makes it particularly important to design control pulses in a robust manner so that the electron shuttling process is insensitive to these parameter uncertainties. We formulate this here as an optimal control problem on the special unitary Lie group. We then discretize the uncertainty range and obtain a finite collection of state transfer problems, each of which takes a different value of the uncertainty parameter. The gradients of the aggregate fidelity with respect to these control fields are then derived in an analytic form, which allows for efficient implementations of gradient types of optimization algorithms. We demonstrate the efficiency of our algorithm here by numerical studies with realistic physical parameters relevant to the electron shuttling between phosphorus dopant ions in silicon.

II. PROBLEM FORMULATION

In this section we provide a general mathematical description for electron shuttling in solid state devices, together with the key associated mathematical background.

The underlying physics and potential applications of

solid state devices with qubits have been widely discussed in the physical community. See, *e.g.*, Refs. [10–12]. For a complete quantum description of the system under realistic conditions, it is necessary to employ the density operator ρ, which is a Hermitian matrix with unit trace. The diagonal elements of the density operator correspond to the electron populations on each site. The dynamics of the density operator is determined by the Liouville-von Neumann equation:

$$\dot{\rho} = -[iH, \rho], \tag{1}$$

where H is a traceless Hermitian matrix which is termed the system Hamiltonian. To be specific, we focus here on a triple donor system, but note that the development and solution shown here can be easily extended to devices with more donors. In this case, the term iH is defined on the Lie algebra $\mathfrak{su}(3)$, *i.e.*, all the 3×3 skew-Hermitian matrices. In Ref. [10], an electron is moved between ends of a chain of ionized phosphorus dopants, for which the Hamiltonian is given by (setting $\hbar = 1$):

$$H = \begin{bmatrix} 0 & -\Omega_{12} & 0 \\ -\Omega_{12} & \Delta & -\Omega_{23} \\ 0 & -\Omega_{23} & 0 \end{bmatrix}. \tag{2}$$

Here Δ is the energy difference between eigenstates, and Ω_{12} and Ω_{23} are the coherent tunneling amplitudes between eigenstates.

Define a basis for $\mathfrak{su}(3)$ as

$$\begin{aligned} X_1 &= \begin{bmatrix} 0 & i & 0 \\ i & 0 & 0 \\ 0 & 0 & 0 \end{bmatrix}, \quad X_2 = \begin{bmatrix} 0 & 0 & 0 \\ 0 & 0 & i \\ 0 & i & 0 \end{bmatrix}, \\ X_3 &= \begin{bmatrix} 0 & 0 & 1 \\ 0 & 0 & 0 \\ -1 & 0 & 0 \end{bmatrix}, \quad X_4 = \begin{bmatrix} 0 & 1 & 0 \\ -1 & 0 & 0 \\ 0 & 0 & 0 \end{bmatrix}, \\ X_5 &= \begin{bmatrix} 0 & 0 & 0 \\ 0 & 0 & 1 \\ 0 & -1 & 0 \end{bmatrix}, \quad X_6 = \begin{bmatrix} 0 & 0 & i \\ 0 & 0 & 0 \\ i & 0 & 0 \end{bmatrix}, \\ X_7 &= \begin{bmatrix} i & 0 & 0 \\ 0 & -i & 0 \\ 0 & 0 & 0 \end{bmatrix}, \quad X_8 = \frac{1}{\sqrt{3}} \begin{bmatrix} i & 0 & 0 \\ 0 & i & 0 \\ 0 & 0 & -2i \end{bmatrix}. \end{aligned} \tag{3}$$

With a rearrangement of order, this choice of $\mathfrak{su}(3)$ basis is seen to be equivalent to the Gell-Mann matrices [16]. In this basis, the Hamiltonian in Eq. (2) can be represented as

$$iH = -\Omega_{12}X_1 - \Omega_{23}X_2 - \frac{\Delta}{2}X_7 + \frac{\Delta}{2\sqrt{3}}X_8 + \frac{\Delta}{3}I_3, \tag{4}$$

where I_3 is the 3×3 identity matrix. We can drop the term $\frac{\Delta}{3}I_3$ since it commutes with all the other terms and thus contributes only a global phase.

Without loss of generality, let us denote the spatial state of the left end of the chain as

$$\rho_I = \begin{bmatrix} 1 & 0 & 0 \\ 0 & 0 & 0 \\ 0 & 0 & 0 \end{bmatrix} \tag{5}$$

and the right end of the chain as

$$\rho_T = \begin{bmatrix} 0 & 0 & 0 \\ 0 & 0 & 0 \\ 0 & 0 & 1 \end{bmatrix}. \tag{6}$$

The electron shuttling can now be formulated as a steering problem, that is, for the dynamical system of Eq. (1), we will apply coherent tunneling amplitudes Ω_{12} and Ω_{23} as control fields to transfer the density matrix ρ from the initial state ρ_I at the initial time $t = 0$ to the final state ρ_T at the terminal time $t = T$.

For a fixed energy difference Δ, this problem has been solved by the same authors in [15]. In that work we developed an efficient numerical algorithm by using the Lie-Poisson reduction theorem. However, as noted above, in real experiments, it is often the case that the exact value of Δ cannot be determined precisely, e.g., due to imperfections in engineering implementations. Instead, we may only know that the energy difference Δ lies in a range $[\Delta^* - \Delta_\epsilon, \Delta^* + \Delta_\epsilon]$, where Δ^* is the nominal value and Δ_ϵ is the maximum possible error bound. These two values are usually available for a specific physical system.

In the rest of this paper, we will design robust control pulses that can achieve the desired spatial state transfer *regardless* of what the true energy difference is in the given interval.

III. ROBUST OPTIMAL CONTROL ALGORITHM

To solve the aforementioned robust state transfer problem, we take a number of sampling points in the uncertainty interval and then form a collection of state transfer problems, each of which has a different energy difference. We then apply a gradient algorithm to find the optimal solution that solves all these problems simultaneously.

To this end, we take N equally spaced points $\{\Delta_n\}_{n=1}^N$ in the uncertainty interval $[\Delta^* - \Delta_\epsilon, \Delta^* + \Delta_\epsilon]$, that is,

$$\Delta_n = \Delta^* - \Delta_\epsilon + \frac{2(n-1)}{N-1}\Delta_\epsilon,$$

and $\Delta_1 = \Delta^* - \Delta_\epsilon$, $\Delta_N = \Delta^* + \Delta_\epsilon$. For each Δ_n, we consider a dynamical system with the Liouville-von Neumann equation

$$\dot{\rho}_n = -[iH_n, \rho_n], \tag{7}$$

where the Hamiltonian H_n is given by

$$iH_n = -\Omega_{12}X_1 - \Omega_{23}X_2 - \frac{\Delta_n}{2}X_7 + \frac{\Delta_n}{2\sqrt{3}}X_8. \tag{8}$$

We now have a set of N dynamical systems, which are all identical except for a different value of Δ in each case.

We want to steer all these N dynamical systems from the initial condition ρ_I in Eq. (5) to the final state ρ_T in Eq. (6). Denote the state trajectory of n-th system as

ρ_n. We can formulate the state transfer for this system as the following minimization problem:

$$\min L_n = \|\rho_T - \rho_n(T)\|_F^2, \tag{9}$$

where the Frobenius norm is defined as

$$\|A\|_F^2 = \mathrm{Tr}\, AA^\dagger. \tag{10}$$

We then have

$$\begin{aligned} L_n =& \mathrm{Tr}(\rho_T - \rho_n(T))(\rho_T - \rho_n(T))^\dagger \\ =& \mathrm{Tr}\,\rho_T\rho_T^\dagger + \mathrm{Tr}\,\rho_n(T)\rho_n^\dagger(T) \\ & - \mathrm{Tr}\,\rho_T\rho_n^\dagger(T) - \mathrm{Tr}\,\rho_n(T)\rho_T^\dagger. \end{aligned}$$

It is easy to show that $\rho = \rho^\dagger$ and $\mathrm{Tr}\,\rho_n(T)\rho_n^\dagger(T) = 1$, and thus minimizing L_n amounts to maximizing the following fidelity function

$$\max J_n = \mathrm{Tr}\,\rho_T\rho_n(T). \tag{11}$$

The robust state transfer can now be formulated as maximization of the aggregate fidelity of all the terminal states $\rho_n(T)$:

$$\max J = \sum_{n=1}^{N} J_n = \sum_{n=1}^{N} \mathrm{Tr}\,\rho_T\rho_n(T). \tag{12}$$

A. Discretization of sinusoidal control fields

As discussed earlier, we use the coherent tunneling amplitudes Ω_{12} and Ω_{23} as control fields. In real physical experiments, there usually exist maximum frequency limits on the control signals. We therefore express the control fields as a finite summation of harmonics:

$$\begin{aligned} \Omega_{12}(t) &= a_0 + \sum_{m=1}^{M}[a_m \cos m\omega t + b_m \sin m\omega t], \\ \Omega_{23}(t) &= c_0 + \sum_{m=1}^{M}[c_m \cos m\omega t + d_m \sin m\omega t], \end{aligned} \tag{13}$$

where $\omega = 2\pi/T$. Here the expansions are truncated at a value M, which can be chosen so that $M\omega$ stays within the feasible frequency range. In the case when M is sufficiently large, Eq. (13) can approximate any continuous control function.

For time varying control fields, there is generally no analytic method to solve the Liouville-von Neumann equation Eq. (7). To obtain numerical solutions, a common practice is to divide the total time duration into a number of small time steps and assume that the control functions are constant within each step. In particular, for a given time duration $[0, T]$, divide it into K equal intervals $\{[t_k, t_{k+1}]\}_{k=0}^{K-1}$ of length $\Delta t = t_{k+1} - t_k = T/K$, where $t_k = k\Delta t$. On each of these intervals $[t_k, t_{k+1}]$, assume the control fields in Eq. (13) take constant values which are equal to those on the left boundary $t = t_k$:

$$\begin{aligned} \Omega_{12}(k) &= a_0 + \sum_{m=1}^{M}\left[a_m \cos mk\frac{2\pi}{K} + b_m \sin mk\frac{2\pi}{K}\right], \\ \Omega_{23}(k) &= c_0 + \sum_{m=1}^{M}\left[c_m \cos mk\frac{2\pi}{K} + d_m \sin mk\frac{2\pi}{K}\right]. \end{aligned} \tag{14}$$

From Eq. (8), we obtain

$$iH_n(k) = -\Omega_{12}(k)X_1 - \Omega_{23}(k)X_2 - \frac{\Delta_n}{2}X_7 + \frac{\Delta_n}{2\sqrt{3}}X_8. \tag{15}$$

Since $iH_n(k)$ is constant on the interval $[t_k, t_{k+1}]$, we can compute its unitary propogator as

$$U_n(k) = e^{-iH_n(k)\Delta t}. \tag{16}$$

It follows that the density operator at the final time can be calculated as

$$\rho_n(T) = U_n(K-1)\cdots U_n(0)\rho_I U_n^\dagger(0)\cdots U_n^\dagger(K-1). \tag{17}$$

To realize the desired robust spatial state transfer, we now only need to maximize the aggregate fidelity in Eq. (12) with respect to the expansion coefficients a_m, b_m, c_m, and d_m in Eq. (13).

B. Gradient derivations

We want to apply a gradient algorithm to find the maximizing expansion coefficients. To this end, we need to calculate the derivatives of the cost function J with respect to those expansion coefficients.

For the ease of notation, let

$$\begin{aligned} \Omega_{12} &= \begin{bmatrix}\Omega_{12}(0) & \cdots & \Omega_{12}(K-1)\end{bmatrix}^T, \\ \Omega_{23} &= \begin{bmatrix}\Omega_{23}(0) & \cdots & \Omega_{23}(K-1)\end{bmatrix}^T, \\ p &= \begin{bmatrix}a_0 & a_1 & \cdots & a_M & b_1 & \cdots & b_M\end{bmatrix}^T, \\ q &= \begin{bmatrix}c_0 & c_1 & \cdots & c_M & d_1 & \cdots & d_M\end{bmatrix}^T, \\ v_K &= \begin{bmatrix}0 & 1 & \cdots & K-1\end{bmatrix}^T, \\ v_M &= \begin{bmatrix}1 & \cdots & M\end{bmatrix}^T. \end{aligned} \tag{18}$$

Then the control fields in Eq. (14) can be rewritten in the following vector form:

$$\begin{aligned} \Omega_{12}(k) &= \left[1 \;\; \cos\left(kv_M^T\frac{2\pi}{K}\right) \;\; \sin\left(kv_M^T\frac{2\pi}{K}\right)\right]p, \\ \Omega_{23}(k) &= \left[1 \;\; \cos\left(kv_M^T\frac{2\pi}{K}\right) \;\; \sin\left(kv_M^T\frac{2\pi}{K}\right)\right]q, \end{aligned} \tag{19}$$

where the matrix functions $\cos(\cdot)$ and $\sin(\cdot)$ are calculated element-wise. Define

$$G = \left[\mathbf{1} \;\; \cos\left(v_K v_M^T\frac{2\pi}{K}\right) \;\; \sin\left(v_K v_M^T\frac{2\pi}{K}\right)\right],$$

where $\mathbf{1}$ is a column vector with all entries being 1. Then we have

$$\Omega_{12} = Gp, \quad \Omega_{23} = Gq. \tag{20}$$

Now the optimization variables become two vectors p and q, both of which lie in $\mathbb{R}^{M+1}$. We proceed to derive the gradients of the aggregate fidelity J with respect to p and q. From Eqs. (12) and (20), we have

$$\frac{dJ}{dp} = \left(\frac{d\Omega_{12}}{dp}\right)^T \frac{dJ}{d\Omega_{12}} = G^T \sum_{n=1}^{N} \frac{dJ_n}{d\Omega_{12}}.$$

Similarly,

$$\frac{dJ}{dq} = G^T \sum_{n=1}^{N} \frac{dJ_n}{d\Omega_{23}}.$$

Next we need to derive $\frac{dJ_n}{d\Omega_{12}(k)}$ and $\frac{dJ_n}{d\Omega_{23}(k)}$. Define

$$\begin{aligned}
\rho_n(k) &= U_n(k-1)\cdots U_n(0)\rho_I U_n^\dagger(0)\cdots U_n^\dagger(k-1),\\
\Lambda_n(k) &= U_n^\dagger(k)\cdots U_n^\dagger(K-1)\rho_T U_n(K-1)\cdots U_n(k),
\end{aligned}$$

where $U_n(k)$ is defined in Eq. (16), and $k = 0, \ldots, K-1$. In addition, define $\rho_n(0) = \rho_I$ and $\Lambda_n(K) = \rho_T$. Then

$$\begin{aligned}
J_n &= \operatorname{Tr}\Lambda_n(K)\rho_n(K) = \operatorname{Tr}\Lambda_n(K-1)\rho_n(K-1)\\
&= \cdots = \operatorname{Tr}\Lambda_n(1)\rho_n(1) = \operatorname{Tr}\Lambda_n(0)\rho_n(0).
\end{aligned}$$

It follows that

$$\begin{aligned}
&\frac{dJ_n}{d\Omega_{12}(k)} = \frac{d\operatorname{Tr}\Lambda_n(k+1)\rho_n(k+1)}{d\Omega_{12}(k)}\\
=&\frac{d\operatorname{Tr}\Lambda_n(k+1)U_n(k)\rho_n(k)U_n^\dagger(k)}{d\Omega_{12}(k)}\\
=&\operatorname{Tr}\Lambda_n(k+1)\\
&\times\left(\frac{dU_n(k)}{d\Omega_{12}(k)}\rho_n(k)U_n^\dagger(k) + U_n(k)\rho_n(k)\frac{dU_n^\dagger(k)}{d\Omega_{12}(k)}\right).
\end{aligned}$$

Using the following expression for the derivative of a matrix exponential [17],

$$\left.\frac{d}{dv}e^{-i(H_a+vH_b)t}\right|_{v=0} = -i\int_0^t e^{-iH_a\tau}H_b e^{iH_a\tau}d\tau\ e^{-iH_a t}, \tag{21}$$

we obtain

$$\frac{dU_n(k)}{d\Omega_{12}(k)} = \int_0^{\Delta t} e^{-iH_n(k)\tau}X_1 e^{iH_n(k)\tau}d\tau\ U_n(k). \tag{22}$$

Substituting Eq. (22) into (21), we get

$$\begin{aligned}
&\frac{dJ_n}{d\Omega_{12}(k)}\\
&= \operatorname{Tr}\Lambda_n(k+1)\left(\int_0^{\Delta t} e^{-iH_n(k)\tau}X_1 e^{iH_n(k)\tau}d\tau\rho_n(k+1)\right.\\
&\qquad\left.-\rho_n(k+1)\int_0^{\Delta t} e^{-iH_n(k)\tau}X_1 e^{iH_n(k)\tau}d\tau\right)\\
&= \operatorname{Tr}[\rho_n(k+1),\Lambda_n(k+1)]\int_0^{\Delta t} e^{-iH_n(k)\tau}X_1 e^{iH_n(k)\tau}d\tau.
\end{aligned} \tag{23}$$

We can further simplify the calculation of Eq. (23). We first note that since $H_n(k)$ is a Hermitian matrix, it can be diagonalized as

$$H_n(k) = T_n(k)\Gamma_n(k)T_n^\dagger(k), \tag{24}$$

where

$$\begin{aligned}
\Gamma_n(k) &= \operatorname{diag}\{\gamma_n^1(k),\gamma_n^2(k),\gamma_n^3(k)\}\\
&= \operatorname{diag}\left\{-\frac{\Delta_n}{3}, \frac{\Delta_n+3g_n(k)}{6}, \frac{\Delta_n-3g_n(k)}{6}\right\},
\end{aligned}$$

and the unitary matrix $T_n(k)$ can be written as

$$T_n(k) = \begin{bmatrix}
-\Omega_{23}(k)/h(k) & \Omega_{12}(k)/\sqrt{g_n(k)(g_n(k)+\Delta_n)/2} & \Omega_{12}(k)/\sqrt{g_n(k)(g_n(k)-\Delta_n)/2}\\
0 & -\sqrt{(g_n(k)+\Delta_n)/(2g_n(k))} & \sqrt{(g_n(k)-\Delta_n)/(2g_n(k))}\\
\Omega_{12}(k)/h(k) & \Omega_{23}(k)/\sqrt{g_n(k)(g_n(k)+\Delta_n)/2} & \Omega_{23}(k)/\sqrt{g_n(k)(g_n(k)-\Delta_n)/2)}
\end{bmatrix},$$

and

$$\begin{aligned}
g_n(k) &= \sqrt{\Delta_n^2 + 4\Omega_{23}^2(k) + 4\Omega_{12}^2(k)},\\
h(k) &= \sqrt{\Omega_{23}^2(k) + \Omega_{12}^2(k)}.
\end{aligned}$$

Therefore we can write,

$$\begin{aligned}
&\int_0^{\Delta t} e^{-iH_n(k)\tau}X_1 e^{iH_n(k)\tau}d\tau\\
=&\int_0^{\Delta t} T_n(k)e^{-i\Gamma_n(k)\tau}T_n^\dagger(k)X_1T_n(k)e^{i\Gamma_n(k)}T_n^\dagger(k)d\tau\\
=&T_n(k)\int_0^{\Delta t}(T_n^\dagger(k)X_1T_n(k))\odot\Psi_n(k)d\tau\ T_n^\dagger(k),
\end{aligned} \tag{25}$$

where $\odot$ denotes the Hadamard product, *i.e.*, element-wise product, of two matrices, and the ab-th element of $\Psi_n(k)$ is $\exp\{i(\gamma_n^b(k) - \gamma_n^a(k))\tau\}$. Now define a matrix $\Phi_n(k)$, whose ab-th element is given by

$$\Phi_n^{ab}(k) = \int_0^{\Delta t} \Psi_n^{ab}(k) d\tau = \begin{cases} \dfrac{\exp\{i(\gamma_n^b(k) - \gamma_n^a(k))\Delta t\} - 1}{i(\gamma_n^b(k) - \gamma_n^a(k))}, & \text{for } a \neq b. \\ \Delta t, & \text{for } a = b. \end{cases}$$

This allows Eq. (25) to be calculated explicitly:

$$\begin{aligned} &\int_0^{\Delta t} e^{-iH_n(k)\tau} X_1 e^{iH_n(k)\tau} d\tau \\ =&T_n(k)((T_n^\dagger(k) X_1 T_n(k)) \odot \Phi_n(k)) T_n^\dagger(k), \end{aligned} \tag{26}$$

which in turn yields that

$$\begin{aligned} &\frac{dJ_n}{d\Omega_{12}(k)} \\ &= \mathrm{Tr}([\rho_n(k), \Lambda_n(k)] T_n(k)((T_n^\dagger(k) X_1 T_n(k)) \odot \Phi) T_n^\dagger(k)). \end{aligned} \tag{27}$$

A similar analysis leads to

$$\begin{aligned} &\frac{dJ_n}{d\Omega_{23}(k)} \\ &= \mathrm{Tr}([\rho_n(k), \Lambda_n(k)] T_n(k)((T_n^\dagger(k) X_2 T_n(k)) \odot \Phi) T_n^\dagger(k)). \end{aligned} \tag{28}$$

We have derived closed form formulae for dJ/dp and dJ/dq, *i.e.*, the gradients of the aggregate fidelity J with respect to the expansion coefficient vectors p and q. It is now straightforward to implement gradient types of algorithms such as the gradient descent algorithm, the conjugate gradient algorithm, or the BFGS algorithm [18].

IV. NUMERICAL OPTIMIZATION

In this section we apply the gradients derived in the preceding section to design the robust control fields that can realize the desired population transfer in solid state devices.

We consider the ionized donor chain that was discussed in Ref. [10]. Typical values of the energy difference Δ are several meV, while the control fields Ω_{12} and Ω_{23} can be varied in the magnitude of 10^{-2} meV. Realistic parameter values allow us to assume a nominal value for Δ^* of 2.72 meV, with the actual value of Δ deviating from the nominal value by up to 20%. We further assume that the population transfer needs to be accomplished within 100 ns, and the maximum feasible frequency for control fields is 0.1 GHz. These constraints lead to the control field expansions in Eq. (14) needing to be truncated at $M = 10$.

We now discretize the total time duration $[0, 100]$ ns into 100 small time steps, each with length 1 ns. Take

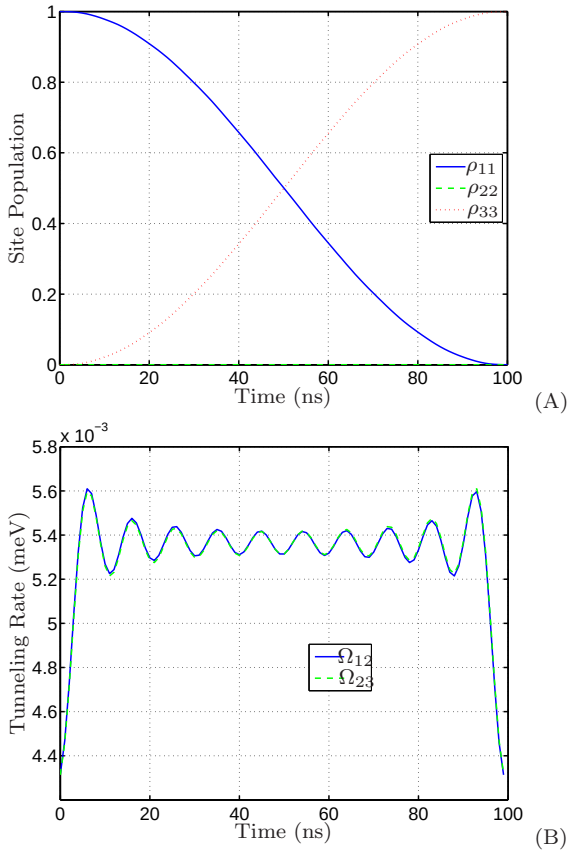

FIG. 1: Control pulses obtained with no robust design. (A) Spatial state transfer when $\Delta = \Delta^* = 2.72$ meV. (B) Control pulses: blue solid line corresponds to Ω_{12}, green dashed line to Ω_{23}. (See electronic version for color plots).

11 evenly distributed sampling points from the uncertainty range $[0.8\Delta^*, 1.2\Delta^*]$ meV. Given these parameter settings, we can apply a gradient algorithm with fixed step size to solve for the optimal control pulses.

As a reference, we first consider the case with no robust design, *i.e.*, optimizing for the point $\Delta = \Delta^*$ only. The corresponding population transfer and control fields are shown in Fig. 1(A) and (B), respectively. To test the robustness, we apply these control pulses to all 11 sampling points in the uncertainty range $[0.8\Delta^*, 1.2\Delta^*]$ meV. The results of these simulations are plotted in Fig. 2. It is evident that when the actual value of Δ is unknown within this range, the electron cannot be successfully transferred from left to right, except in the case when (coincidentally) $\Delta = \Delta^*$. Note that in each of the unsuccessful transfers, a full transfer is achieved at some point before the final time T. However, the oscillatory nature of the populations leads to a reversal of the transfer. Therefore, experimentally, a number of different transfer times would have to be attempted for a given pulse sequence in order to assess the possibility of a complete transfer and to determine the optimal time. Furthermore, noise in any element of the Hamiltonian may cause the optimal transfer time for a given pulse sequence to be different

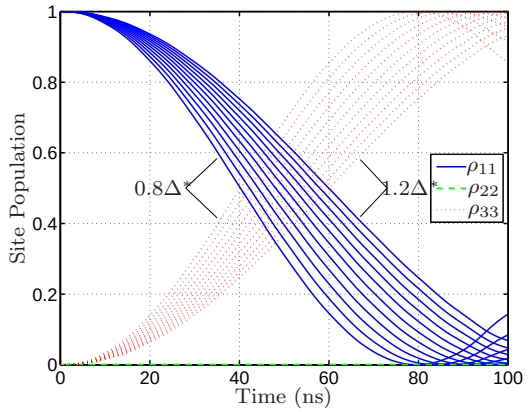

FIG. 2: Robustness test for the control pulses in Fig. 1: spatial state transfers for 11 evenly distributed Δ's in the range $[0.8\Delta^*, 1.2\Delta^*]$, where $\Delta^* = 2.72$ meV.

for each individual experiment.

Next we apply the robust control pulses design developed above. The optimization results for this scheme are shown in Fig. 3. The robust controls are seen to be about an order of magnitude larger than the controls for Δ^* only. Most importantly, it is clear that whatever value of energy difference Δ within the $\pm 20\%$ deviation range of the nominal value $\Delta^* = 2.72$ meV is employed, the resulting robust control fields can transfer the population with almost perfect fidelity. The robust controls also have the advantage that the populations do not oscillate as in Fig. 2. Slight changes in transfer time would therefore not affect the population transfer, a useful robustness feature from the experimental perspective. Finally, we note these pulses also perform well outside the range for which they were defined. For example, if the real uncertainty level is $\pm 25\%$ instead of $\pm 20\%$ in the design, the spatial state transfer still has acceptable performance, as shown in Fig. 4.

V. CONCLUSION

In this paper we have formulated robust control pulses designed for electron shuttling in a chain of donors as a collection of state transfer problems, each of which corresponds to a different value in the uncertainty parameter range. We derived explicit formulae for the gradients of the aggregate fidelity with respect to the control fields, and then applied a direct gradient algorithm to solve this problem efficiently. The results for electron shuttling across a three site chain show that the robust design significantly improves the performance of an electron shuttling protocol, achieving near perfect state transfer across a realistic range of Hamiltonian parameters for a phosphorus-doped silicon system.

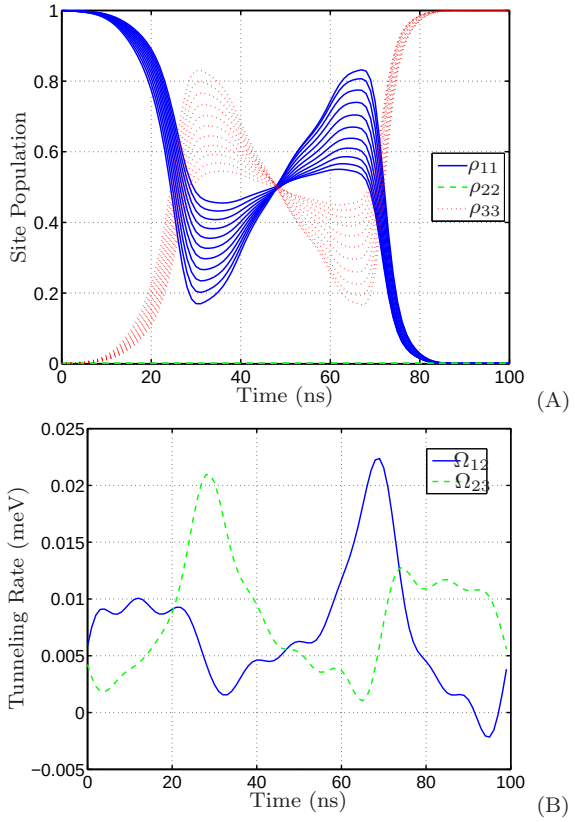

FIG. 3: Design of robust control fields. (A) Spatial transfer for 11 evenly distributed values of Δ's in the range $[0.8\Delta^*, 1.2\Delta^*]$, where $\Delta^* = 2.72$ meV. (B) Robust control pulses: blue solid line corresponds to Ω_{12}, green dashed line to Ω_{23}. (See electronic version for color plots).

Acknowledgments

JZ thanks the financial support from the Innovation Program of Shanghai Municipal Education Commission under Grant No. 11ZZ20, Shanghai Pujiang Program under Grant No. 11PJ1405800, NSFC under Grant No. 61174086, and State Key Lab of Advanced Optical Communication Systems and Networks, SJTU, China. XD thanks the University of California-Berkeley College of Chemistry Summer Research Stipend. We thank NSA (Grant No. MOD713106A) for financial support.

[1] B. E. Kane, Nature **393**, 133 (1998).
[2] A. J. Skinner, M. E. Davenport, and B. E. Kane, Phys. Rev. Lett. **90**, 087901 (2003).
[3] J. J. L. Morton, D. R. McCamey, M. A. Eriksson, and S. A. Lyon, Nature **479**, 345 (2011).
[4] R. Vrijen, E. Yablonovitch, K. Wang, H. W. Jiang, A. Ba-

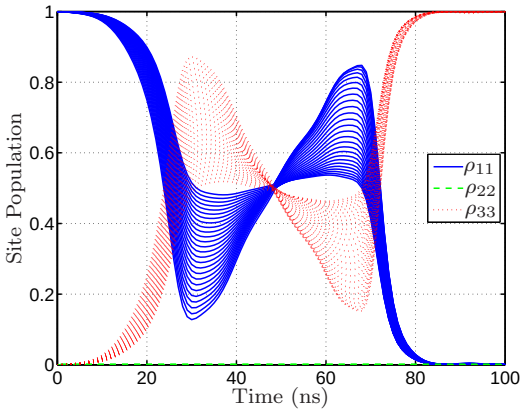

FIG. 4: Robustness test for ±25% uncertainty level: spatial state transfers for 11 evenly distributed Δ's in the range $[0.75\Delta^*, 1.25\Delta^*]$, where $\Delta^* = 2.72$ meV. (See electronic version for color plots).

landin, V. Roychowdhury, T. Mor, and D. DiVincenzo, Phys. Rev. A **62**, 012306 (2000).

[5] S. Goswami, K. A. Slinker, M. Friesen, L. M. McGuire, J. L. Truitt, C. Tahan, L. J. Klein, J. O. Chu, P. M. Mooney, D. W. van der Weide, et al., Nature Physics **3**, 41 (2007).

[6] T. Schenkel, A. Persaud, S. J. Park, J. Nilsson, J. Bokor, J. A. Liddle, R. Keller, D. H. Schneider, D. W. Cheng, and D. E. Humphries, J. Appl. Phys. **94**, 7017 (2003).

[7] S. E. S. Andresen, R. Brenner, C. J. Wellard, C. Yang, T. Hopf, C. C. Escott, R. G. Clark, A. S. Dzurak, D. N. Jamieson, and L. C. L. Hollenberg, Nano Lett. **7**, 2000 (2007).

[8] A. S. Dzurak, A. Morello, M. Y. Simmons, L. C. L. Hollenberg, G. Klimeck, S. Rogge, S. N. Coppersmith, and M. A. Eriksson (2012), arXiv:1206.5202v1.

[9] S. R. Schofield, N. J. Curson, M. Y. Simmons, F. J. Ruess, T. Hallam, L. Oberbeck, and R. G. Clark, Phys. Rev. Lett. **91**, 136104 (2003).

[10] A. D. Greentree, J. H. Cole, A. R. Hamilton, and L. C. L. Hollenberg, Phys. Rev. B **70**, 235317 (2004).

[11] R. Rahman, R. P. Muller, J. E. Levy, M. S. Carroll, G. Klimeck, A. D. Greentree, and L. C. L. Hollenberg, Phys. Rev. B **82**, 155315 (2010).

[12] B. Chen, W. Fan, and Y. Xu, Phys. Rev. A **83**, 014301 (2011).

[13] N. V. Vitanov, T. Halfmann, B. W. Shore, and K. Bergmann, Annual Review of Physical Chemistry **52**, 763 (2001).

[14] K. Bergmann, H. Theuer, and B. W. Shore, Rev. Mod. Phys. **70**, 1003 (1998).

[15] J. Zhang, L. Greenman, X. Deng, and K. B. Whaley (2012), submitted to *Phys. Rev. B*.

[16] H. Georgi, *Lie Algebras In Particle Physics* (Westview Press, 1999), 2nd ed.

[17] I. Najfeld and T. F. Havel, Advances in Applied Mathematics **16**, 321 (1995).

[18] E. Polak, *Optimization: Algorithms and Consistent Approximations* (Springer, 1997).